Available online at www.sciencedirect.com
ScienceDirect
Journal of the European Ceramic Society 28 (2008) 2673–2680
www.elsevier.com/locate/jeurceramsoc

Laser drilling of Ni–YSZ cermets

J. Gurauskis, D. Sola, J.I. Peña, V.M. Orera *

Instituto de Ciencia de Materiales de Aragón, CSIC-Universidad de Zaragoza, C/ Pedro Cerbuna 12, E-50009 Zaragoza, Spain

Received 25 February 2008; accepted 17 April 2008
Available online 4 June 2008

Abstract

Pulsed Nd:YAG laser was used for efficient drilling of cylindrical hole patterns in porous Ni–YSZ cermet plates. Green NiO–YSZ oxide ceramic substrates obtained via tape casting technique were machined using 8–80 ns pulses at the fixed wavelength of 1064 nm. The etched volume, drill diameter, shape and depth were evaluated as a function of the processing parameters such as pulse irradiance and pulse number. The laser machining mechanism was discussed by means of laser–material interaction parameters such as beam absorptivity and plasma formation and the impact to the overall process discussed. Holes with uniform diameter from 30 to 110 μm and up to 1 mm depth were drilled with a high efficiency of up to 0.1 mm^3 per pulse. Green state machining showed significant efficiency whereas the properties of the cermet substrate were kept unchanged.

Keywords: Tape casting; Laser drilling; Transition metal oxides; ZrO_2; Fuel cells

1. Introduction

Ceramics machining with laser is a mature technology that comes from microelectronics industry for scribing an aperture drilling.[1,2] Recent developments and progresses of laser technology have lowered their price and increased their versatility, thus making them an attractive option for a wider range of materials to be processed and machined with.[3,4] Their application to ceramic industry is of particular interest because of the nature of conventional methods used, which are extremely laborious and time-consuming. Furthermore, laser-based machining techniques present unique advantages due to their ability to produce high precision machining with excellent surface quality while yielding small heat affected zones.

Nevertheless the laser machining of ceramics in the sintered state may present some shortcomings due to the presence of spatter and resolidified matter around the hole entrance or microcrack formation resulting from thermal shock.[2,3,5] Heat input can be kept low by using nano-, pico- or femtosecond lasers.[3] However a more efficient approach to ceramic machining is the laser machining of the ceramics in their green state.[1,2,4–7] Green state machining showed to be successful in part by the fact that green ceramics presents lower heat conduction than sintered ceramics. In addition presence of organic matter, as binder or gelling agent, produces a material etching mechanism quite different from that of fired ceramics. In short, the ceramic particles in the green body absorb the laser radiation and heat up significantly, the surrounding organic matter pyrolizes producing a gas jet. The expanding gas jet drags the surrounding matter outside of the processing site. Depending on the laser wavelength used and because of the different threshold fluence between the organic matter and the ceramic particles a "cold" ablation can be achieved. The material being removed with no significant heating of the ceramic.[6] Critical issue on cold ablation processing is the absorption of the laser radiation by the organic compounds.

Previous works with laser drilling of the ceramics in the green state deals mainly with alumina or alumina composite sheets machined with Nd:YAG- or CO_2-pulsed lasers. The wavelength at 1064 nm of Nd:YAG laser for alumina resulted in a better spatial resolution but with relative low removal rate because of the weak absorption.[5] In order to improve the absorption properties of green alumina substrates Slocombe et al.[7] suggested the addition of pigments. A different strategy to increase cold ablation efficiency was used by Nowak et al.[6] They used the CO_2 laser for ablation tests of LTCC composite (20–40 wt.% of Al_2O_3). The presence of such a high amounts of organic matter (26–46 wt.%) permitted to activate the ablation mechanism without presence of any thermal effects within oxide matter.

* Corresponding author. Tel.: +34 976 761333; fax: +34 976 761229.
E-mail address: orera@unizar.es (V.M. Orera).

0955-2219/$ – see front matter © 2008 Elsevier Ltd. All rights reserved.
doi:10.1016/j.jeurceramsoc.2008.04.012

Table 1
Some characteristics of the solid oxide powders used in the study

Powder (manufacturer)	d_{V50} (μm)	ρ_{TD} (g/cm^3)	Absorption coefficient at 1.064 μm
NiO (nickel(II) oxide, Alfa Aesar GMBH, Germany)			
As received	44	6.67	1.520
Milled	1.7	6.67	0.370
ZrO_2 (8 mol% Y_2O_3) (TZ-8YS, TOSOH, Japan)			
As received	0.1	5.9	0.002

The purpose of this work is to produce micron size channels in Ni–YSZ cermets to improve gas permeation. We used a three-step procedure. First, holes were machined in NiO–YSZ green ceramic substrates with an industrial Nd:YAG laser working at the wavelength of 1064 nm. Nd:YAG laser was chosen due to its excellent beam focus ability, precision in machining large areas and accuracy in the iteration of the process. The high absorption of laser radiation by the NiO particles and fast heat transfer to organic binders only present in amounts of 5 wt.% of solids resulted in fast material removal rates. In a second stage the machined NiO–YSZ plates were fired. Porous Ni–YSZ cermets with the desired drilled pattern were produced by reduction of the sintered NiO–YSZ ceramic plates.

2. Experimental

2.1. Preparation of ceramic substrates

The ceramic substrate was prepared using commercial ceramic powders (Table 1) via colloidal processing route based on the tape casting technique. The composition of 71 wt.% NiO and 29 wt.% of 8 mol% yttria-stabilized zirconia (named NiO–YSZ) was used in this study. Prior to the slurry preparation, the nickel oxide powder was attrition milled in organic media during 4 h using zirconium bath (d = 1 mm). The resulted powder showed the mean particle size of 1.7 μm as determined by scanning electron microscope (SEM) measurements. The deionised water was used as a solvent and polyacrylic acid-based polyelectrolyte (PAA, Duramax D-3005, Rohm and Haas, USA) was used as dispersing agent. The ceramic powders were dispersed in solvent using 50 vol.% solids loading with the dispersant concentration of 0.5 wt.%, referred to solids. Obtained suspension was ball milled with a planetary mill during 2 h. Two acrylic polymers were used as binders, a low glass transition temperature binder (Duramax B-1000, Rohm and Haas, USA, $T_g = -26$) and a high glass transition temperature one (Duramax B-1235, Rohm and Haas, USA, $T_g = 14$). The final proportion of binders was 10 wt.% referred to ceramic powder. The suspension was stabilized for 24 h using a low-speed rotating roller. Tape casting was performed on fixed Mylar carrier film using Doctor Blade equipment with the blades gap of 600 μm. After the drying in air for 24 h tapes obtained the final thickness of ≈500 μm and green density of 54% ($\rho_{green} = 3.5 \pm 0.1$ g/cm^3). Some tapes were stacked and cold rolled to obtain the substrates with the desired thickness.

For comparison purposes some substrates were sintered prior to laser machining using single binder burnt out and sintering cycle. Binder burn out was carried out with a heating rate of 1 °C/min up to 600 °C, followed by a dwell time of 30 min. Subsequent sintering was carried out by increasing the temperature with a heating rate of 5 °C/min up to the sintering temperature (1400 °C) with a dwell time of 2 h. Obtained substrates reached 95% of theoretical density ($\rho_{sintered} = 6.2 \pm 0.1$ g/cm^3). Some relevant thermo-physical properties of both green state and sintered NiO–YSZ ceramics are compiled in Table 2.

A reduction cycle of 2 h in a 5 vol.% N_2/H_2 gas mix at 800 °C completely transforms the sintered NiO–YSZ bodies into Ni/YSZ porous cermets of volume composition, 43.5% YSZ, 33.1% metallic Ni and 23.4% pores. According to previous studies on the reduction process in compounds of similar composition, reduction proceeds without a significant microstructure coarsening or sample contraction.[8,9]

2.2. Laser processing of the ceramic substrate

A commercial diode-pumped Nd:YAG laser has been used in this work (Rofin-Sinar E-Line 20). The laser system operates at its fundamental wavelength of 1064 nm with a maximum mean power of 11 W, in a Gaussian beam mode TEM_{00} with a beam quality factor $M^2 < 1.3$. The opto-acoustical Q-Switch commutator controls the cavity output in continuous and in pulsed mode, being generated pulses as short as 8 ns in a frequency rank of 1–40 kHz.

Since we search for a high speed drilling procedure of relatively small holes (less than 100 μm diameter) we used the fixed-beam percussion method instead of trepanning optics method more appropriated for larger diameter holes. The beam

Table 2
Some thermo-physical properties of NiO–YSZ ceramics[10–13]

	Green[a]	Sintered	Cermet
Density, ρ (g/cm^3)	3.5 ± 0.1	6.2 ± 0.1	5.48 ± 0.1
Specific heat, c_p (J/(g K))	0.503	0.503	≈0.5
Thermal conductivity, κ (W/(cm K)) (1000 °C)	0.018	0.033	0.24
Thermal diffusivity, D (cm^2/s) (1000 °C)	7.2×10^{-3}	7.2×10^{-3}	8.7×10^{-2}
Thermal diffusion length, L_{th} (μm) (8 ns pulse)	0.15	0.15	0.53
Vaporization enthalpy, H_v (kJ/cm^3)[b]	18.36	32.3	
Melting temperature, T_M (°C)	1851.58	1851.58	1453.85 Ni, 2676.85 YSZ

[a] 10 wt.% of binder has been discounted. ρ and c_p are taken as mass averages.
[b] From solid phase at 26.85 °C. Mass averages.

Table 3
Laser characteristics for 1 kHz pulse repetition rate

Characteristic	Diode current (A)				
	18[a]	20[a]	23[a]	25	35
Energy per pulse (mJ)	0.1	0.3	0.6	0.9	2.7
Pulse length FWHM (ns)	78	31	25	20	8
Peak power (kW)	4.5	20	35	60	300
Output power (W)	0.1	0.4	0.7	1.0	2.8
Pulse irradiance (GW/cm^2)	0.56	3.08	6.9	10.8	51.0
Thermal penetration depth, L_{th} (μm)[b]	0.47	0.3	0.27	0.24	0.15

[a] Data extrapolated from manufacturer laser characteristics.
[b] From Eq. (1).

was deflected by a programmable galvanometer scanner controlled by a CAD software in such a way that a predefined pattern and processing procedure can be performed. An optical magnifier 5× and a 100 mm optical lens enable laser spots as small as 15 μm in diameter. Being the sample placed at focal distance, it is irradiated by means of pulse bursts. The sample can be properly processed using this method because the laser repetition angular deviation is below 22 μrad. The process is done varying the pulse number and the irradiance per pulse according to the laser output parameters given in Table 3. Laser beam diameter and consequently, laser spot diameter at the material surface depends on diode current. To calculate the laser irradiance at different laser powers we performed laser ablation experiments on methacrylate and taking as laser beam diameter that of the laser imprint after 10 pulses. Modifying the pulse number and the diode current, hence the irradiance of the incoming laser beam, the depth and the diameter of the processed hole can be well-established and controlled.

2.3. Characterization techniques

Scanning electron microscopy was performed using a JEOL JSM6400 microscope. Energy dispersive X-ray analysis (EDAX) was carried out for phase identification. An optical confocal profilometer (OCP) (Dual Sensofar PLμ 2300) with maximum lateral resolution of 0.3 μm was used to analyse the geometrical parameters of the drills. A minimum of 10 drills were measured for each processing variable. A digital camera (Olympus C-310) with capture speed of 8 frames/s was used to estimate plasma geometry. Absorption coefficients in the green ceramics were determined from optical absorption measurements of very thin samples produced by tape casting in a Cary 500 spectrophotometer.

3. Experimental results and discussion

Hole diameter, drilled depth and consequently, drilling efficiencies are very much dependent on laser focussing. In order to compare drilling efficiencies we performed laser drill experiments in tapes of Ni–YSZ, NiO–YSZ sintered and NiO–YSZ green of the same thickness always maintaining the same distance between the surface of the plate and the laser output window.

Direct laser drilling of Ni–YSZ cermets is a very inefficient process and produces holes of poor quality. Fig. 1 shows some pictures of the holes performed by 10 pulses with different laser powers and the hole profiles along the largest section taken with the optical confocal profilometer in a Ni–YSZ cermet plate. The material removal rate is about 1000 μm^3 per pulse and independent of the laser fluence. Besides, the hole shape is irregular with elevated hole borders and debris material left inside the hole. Debris mainly consists of small drops of metallic Ni which is presumably generated by the differential laser evaporation of the cermet components because of the lower melting point of the metallic nickel (see Table 2). Direct drilling of cermets was disregarded due to these problems.

The drilling efficiency of NiO–YSZ substrate was compared between ceramic material in green and sintered state. For this purpose pulses of 2.7 mJ are used. In the case of sintered ceramic substrate the maximum number of pulses ($n = 150$) was insufficient to perforate the tape (thickness ≈ 410 μm). While in the case of green ceramic substrate 50 pulses of the same irradiance were sufficient to generate clean perforation throughout whole tape (thickness ≈ 510 μm). Fig. 2 shows the optical confocal profilometer generated images of drills performed using 25 pulses. The drill in sintered substrate (Fig. 2a) was $h \approx 15$ μm deep and had a diameter of $d \approx 60$ μm with the elevated borders formed from the melted material. While the drill in green substrate (Fig. 2b) was $h \approx 110$ μm deep and had a diameter of $d \approx 90$ μm with borders free of melted material debris.

By observing the results represented in Fig. 2 it is evident that material removal rates for sintered ceramic substrate are very poor, less than 1700 μm^3 per pulse, compared with green ceramic substrate, about 28,000 μm^3 per pulse. Furthermore, the drilling procedure in sintered ceramic substrate resulted in the spatter deposition in nearby zone to the drill. The difference of more than 16 times in drill performance is attributed to the different etching mechanism. In fact, in sintered ceramics the material is removed by the thermal mechanism activated by laser beam. It essentially consists in the absorption of laser energy and subsequent evaporation and ejection of the material. Two critical length scales are of importance here. The optical absorption length defined as $L_\alpha \approx \alpha^{-1}$, α being the absorption coefficient of the ceramics and the thermal diffusion length defined by

$$L_{th} = 2\sqrt{D\tau} \quad (1)$$

where D is the thermal diffusivity and τ is the pulse width. Using Maxwell volumetric averages for thermal conductivity and diffusivity and considering that influence of pores (≈1 μm diameter) is negligible and using data for NiO and YSZ given in Table 2 we obtained the D values of Table 2 and the L_{th} values of Table 3. Optical absorption measurements in very thin plates obtained by tape casting give us an absorption coefficient of 8500 cm^{-1} for NiO–YSZ ceramics. The optical length is about 1.2 μm. Clearly, $L_\alpha > L_{th}$ in all the cases studied in this paper and consequently, drill diameter in sintered ceramics is about the size of the laser beam. Using diffuse reflectance measurements we estimated a reflectance of 0.4 for the ceramics studied.

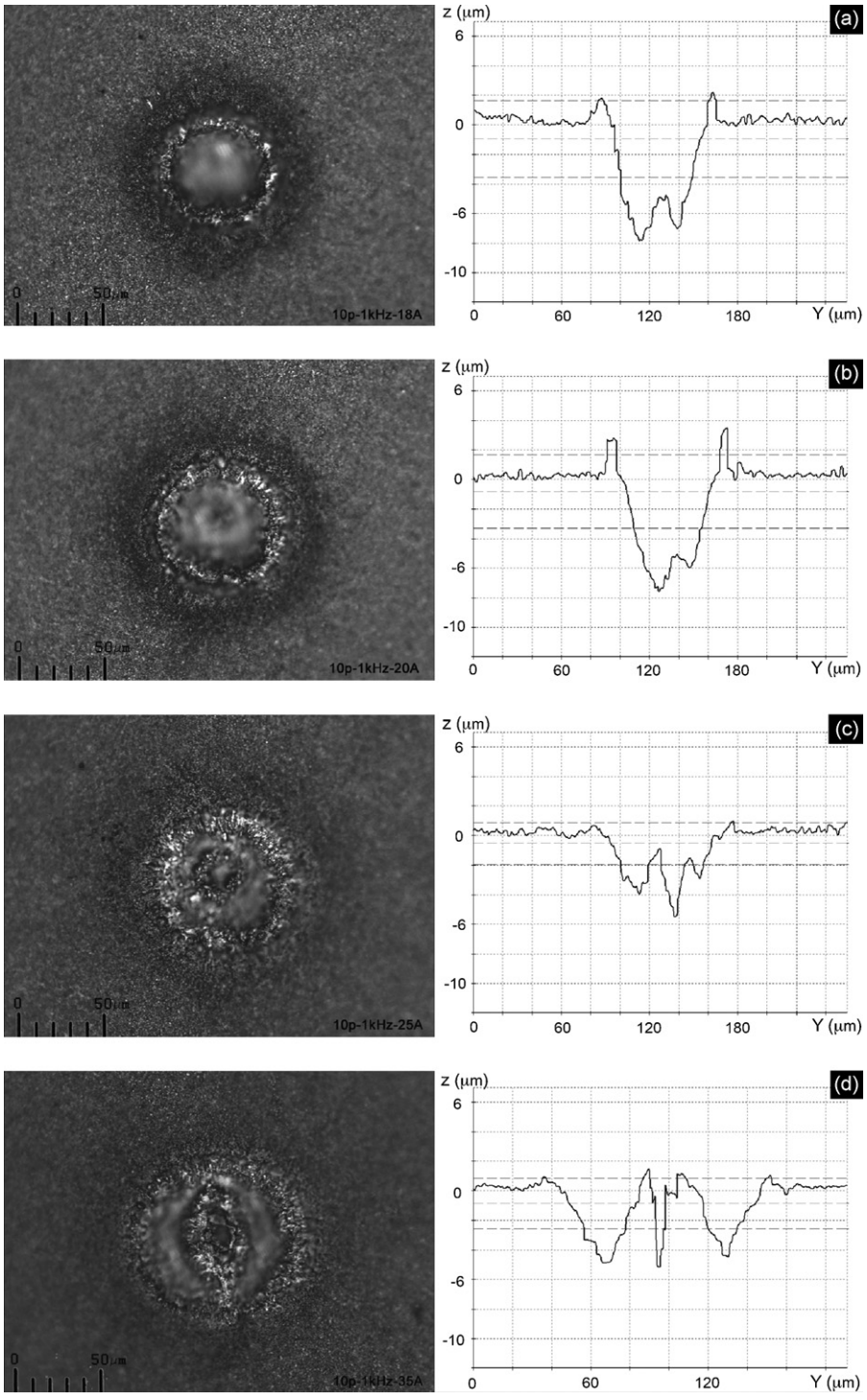

Fig. 1. Holes performed in Ni–YSZ cermet with 10 pulses of (a) 0.1 mJ, (b) 0.3 mJ, (c) 0.9 mJ and (d) 2.7 mJ. Micrographs of the processed surfaces (left hand side) and corresponding profiles (right hand side) measured with an optical profilometer are represented.

In sintered NiO–YSZ ceramics material is removed at an approximate rate of 0.6 μm per pulse that is one half of the estimated laser beam penetration length. Taking into account the etched volume and the energy density per pulse, once the 40% reflection loss was discounted, we obtained a value of 810 kJ/cm^3 for the energy per removed volume. This value is clearly higher than the evaporation enthalpy calculated in Table 2. The difference is attributed not only to optical losses at the surfaces of deflecting mirrors, radiation and convection losses, but to the absorption of the incoming laser beam by the plasma plume.[10]

However, in the case of green ceramic substrate, the drilled depth per pulse is about 5 μm, clearly higher than the estimated optical length. The absorbed energy per etched volume is now 30 kJ/cm^3. The energy losses, which are so important in the sin-

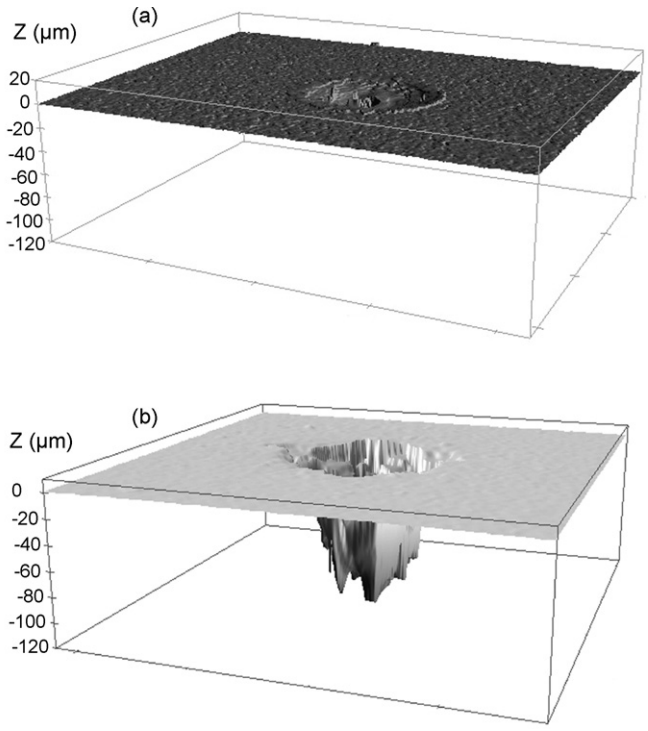

Fig. 2. Optical profilometer generated images of drills obtained using 25, 51 GW/cm^2 pulses in (a) NiO–YSZ sintered ceramic substrate and (b) NiO–YSZ green ceramic substrate.

tered ceramic machining process, are expected to play a similar role here.

Consequently, we conclude that a different etching mechanism governs the green state laser drilling. Results suggest that in the case of green ceramics a new length scale has to be also considered (Fig. 3). We define it as the mechanical length L_m, which accounts for the spallation of ceramic components by fast expanding gases. In fact, laser beam energy is absorbed by organic matter or, in the present case more likely by the strongly absorbing NiO particles, heat is transferred to organics which pyrolizes giving raise to a fast expanding gas jet (Fig. 3c). Mechanical moment transfer from fast expanding gases to ceramic particles produces ejection of ceramic material. Thus, results observed in green ceramics can be understood by the combination of thermal and mechanical processes, being the relevant length scale given by $L_\alpha + L_{th} + L_m$. As it was stated by Knowles et al.[3] this process may result in high etching efficiency values.

Assuming that drill diameter and per pulse depth in the sintered state approximately corresponds to the effective laser beam size, i.e. to $L_\alpha + L_{th}$ in both transverse and longitudinal directions of the hole, we obtain that L_m is about 15 μm along the drill radius and 4 μm in the laser beam direction. Clearly, removal of material by spallation is more efficient in the hole walls than in the hole bottom, due presumably to the pressure of the laser plume.

We have optimised the laser beam focus searching for efficient drilling of green ceramics. The obtained drill geometrical

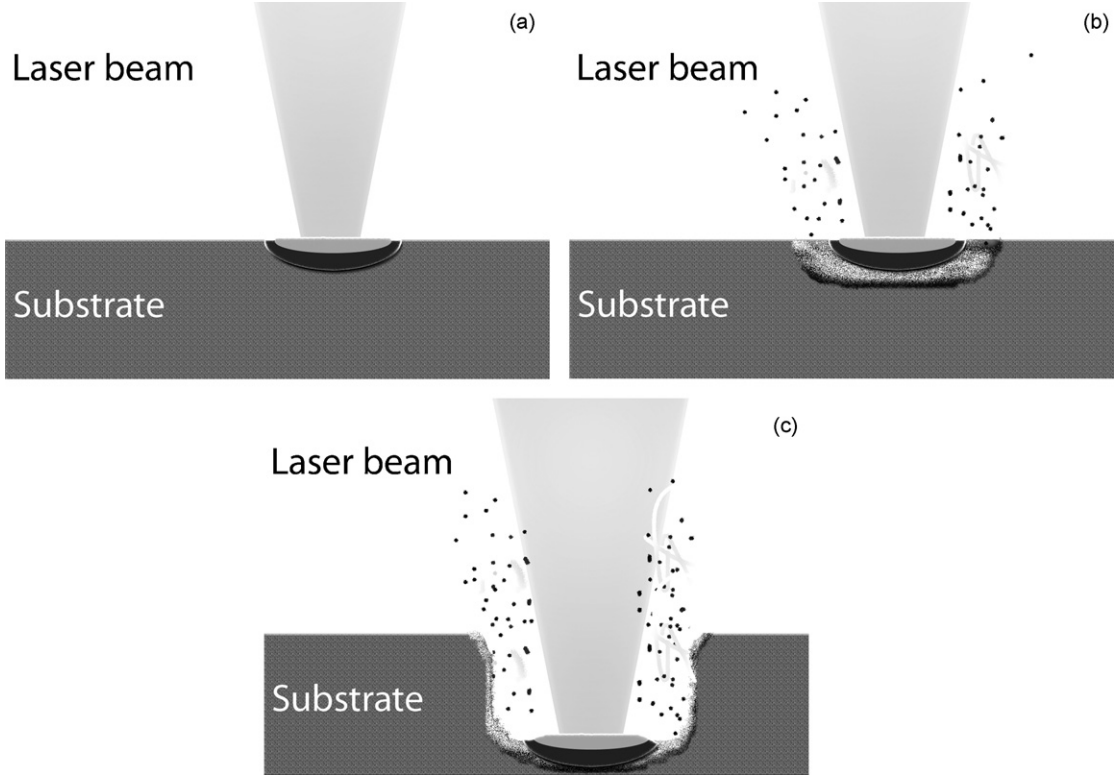

Fig. 3. Proposed schematics of the green state laser drilling in ceramic substrate. (a) Heat is absorbed by ceramic particles and at this point only effective laser beam size ($L_\alpha + L_{th}$) parameters are present. (b) Heat absorbed by ceramic particles is transferred to organics which pyrolizes giving a rise to a gas jet, thus incorporating the mechanical length parameter (L_m). (c) Spallation produced by fast expanding gas jet contributes significantly to the material removal from the drill.

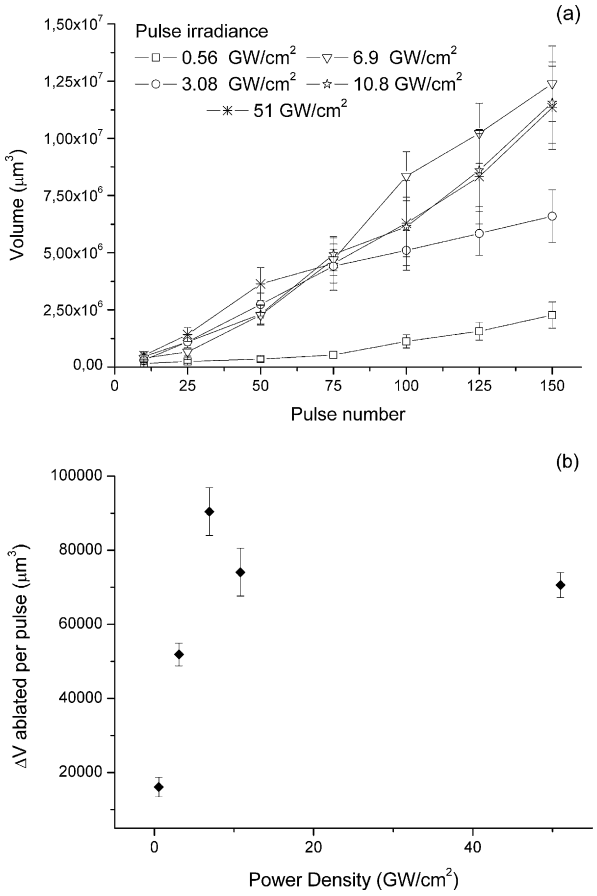

Fig. 4. Drilled volume in green ceramic substrate as a function of the laser irradiance: (a) total drill volume and (b) volume per pulse.

parameters versus pulse number at different laser irradiances are represented in Figs. 4 and 5. Drilled volume (Fig. 4a) increases linearly with number of pulses and the slope gives the etched volume per pulse, $\Delta V/p$, plotted in Fig. 4b as a function of the laser irradiance. It is interesting to notice that $\Delta V/p$ increases with laser beam energy reaching an optimum value at about 6.9 GW/cm^2 of about 90,000 μm^3 per pulse and then decreases slightly with laser power presumably because of the above mentioned plasma absorption.

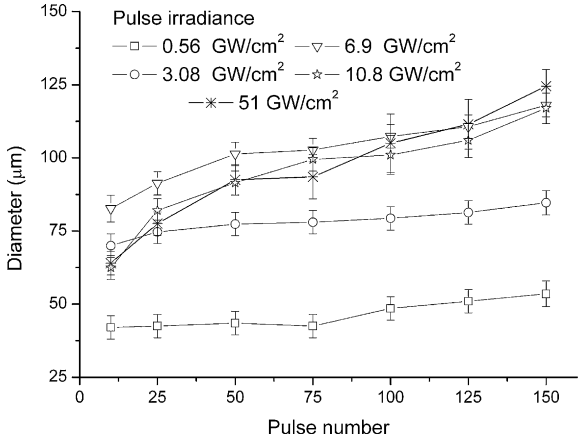

Fig. 5. Drill diameters obtained using varying irradiances per pulse.

Table 4
Pulse irradiances and corresponding plasma diameters measured using digital camera

Pulse irradiance (GW/cm^2)	Plasma diameter (μm)
0.56	360
3.08	560
6.9	760
10.8	1010
51.0	830

On the contrary, drill diameter data represented in Fig. 5 remains essentially constant with pulse number. Drilled diameter increases with laser beam energy for the lowest irradiances used and then saturates around 100 μm for energies above 0.6 mJ. This saturation effect can be attributed to the plasma formation and corresponding shielding mechanism. As it is possible to observe from Table 4, growing pulse irradiances causes the increasing plasma diameter up to irradiance values of 6.24 GW/cm^2, then the plasma diameter growth stabilizes. Further laser energy increase show little effect on the plasma geometry change indicating its full formation and consequent laser beam shielding.

Although for pulses of 0.6 mJ the highest ablation rate is obtained (Fig. 4b) the lowest pulse energy, 0.1 mJ, was selected

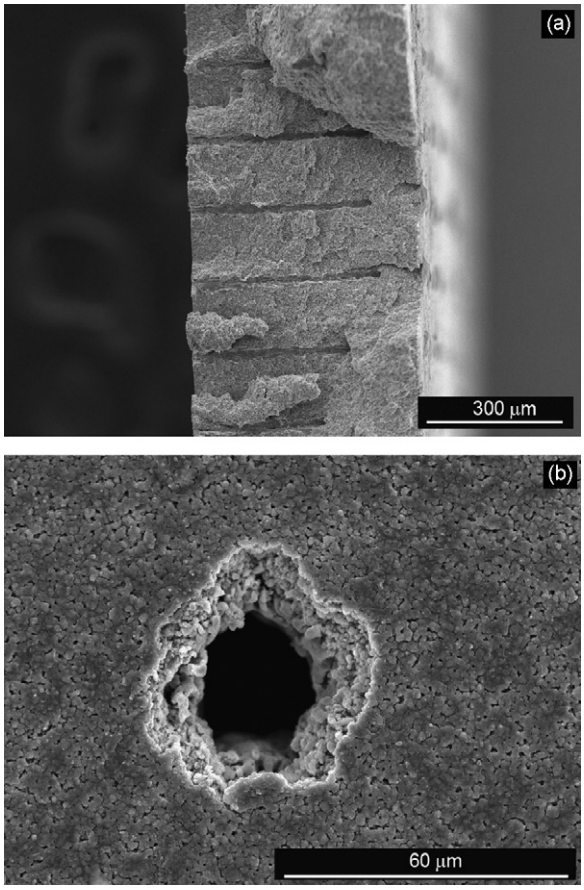

Fig. 6. SEM images of drilling features using 0.56 GW/cm^2 pulses in NiO–YSZ green ceramic substrate: (a) general view of channel revealed on fracture surface and (b) front view of the hole made with 50 pulses.

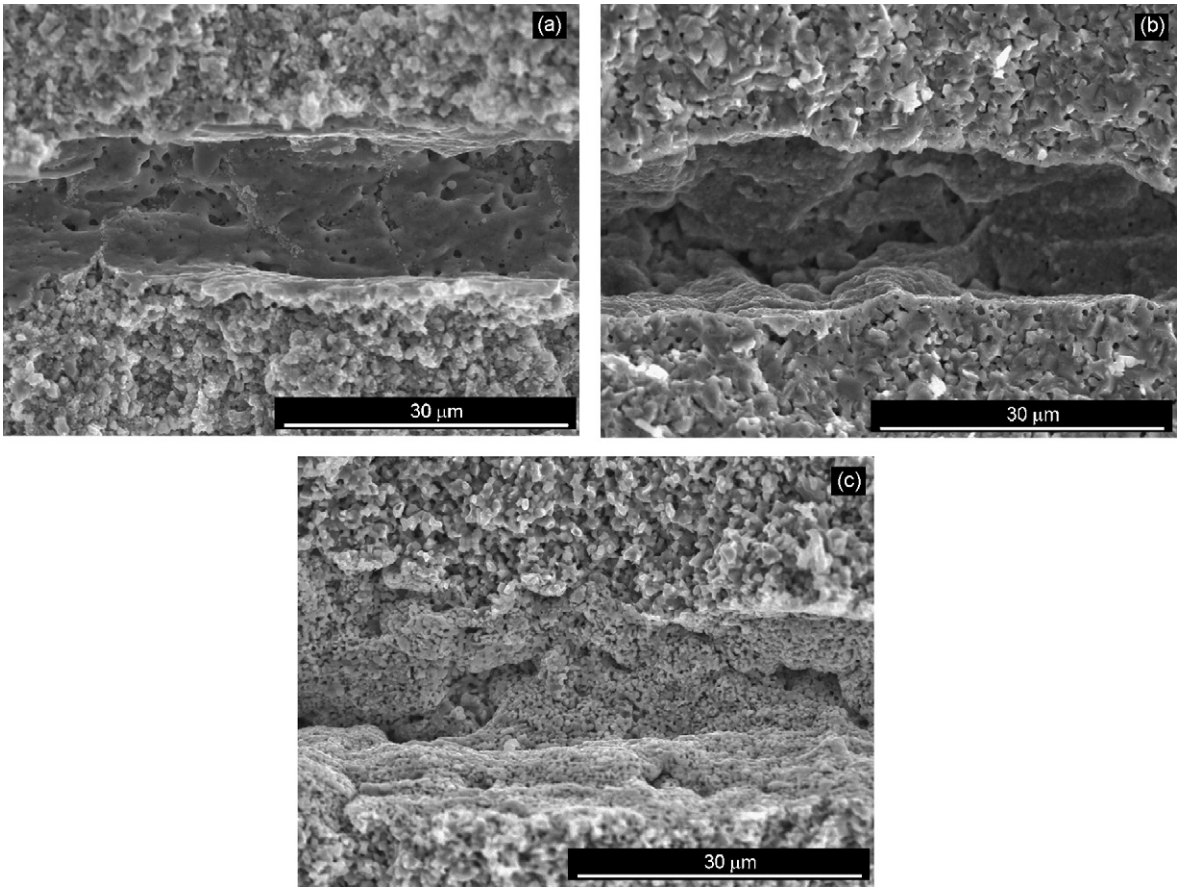

Fig. 7. Cross-section of the drills made with 50, 0.56 GW/cm^2 pulses. SEM micrographs correspond to ceramic substrate in (a) green, (b) as sintered and (c) reduced states.

for further work due to the lowest drill diameter generated at the surface of the substrate throughout whole pulse number range investigated.

Fig. 6 shows the cross-section in fractured surface (Fig. 6a) and the front view (Fig. 6b) of the drills performed in NiO–YSZ substrate using 50 pulses of 0.1 mJ per pulse. As shown in the figure, the drills present a constant diameter throughout the whole drill. Nevertheless, in all the drills studied we find a cone-shaped section at the beginning of the drill, which extends into the substrate to a depth similar to the drill radius. This phenomenon can be attributed to the effect of the ejection gas jet. The pressure supported by the surface increases as the gas reaches the surface, together with the fact that ceramics particles closer to the surface need less momentum to be detached than particles in bulk, generating this conical zone. Much severe features were reported in the works of Imen and Allen[1], Guo et al.[5] and Nowak et al.[6] where drills made with CO_2 laser presented the cone-shaped sections (tapering) almost through out the whole length of the drill.

The cross-section of a drilled hole using 50 pulses of 0.1 mJ per pulse is shown in Fig. 7a. At this magnitude of observation it was possible to detect the presence of a very thin layer of melted material on the wall surface. The EDAX analysis of the layer showed solely the presence of metallic nickel. According to the drill model described before presence of a thin layer of metallic nickel in the walls of the hole may indicate that after laser beam energy is absorbed by NiO particles they reach a temperature high enough to achieve reduction conditions in air atmosphere. Hot metallic particles are projected against the walls producing the observed metallic coating. The presence of the metallic nickel phase layer on the drill walls could lead to undesirable effects in the gas transport between drilled channels and the final product, porous Ni–YSZ cermet. Fig. 7b shows the cross-section of the drill after the sintering stage. The sintering step (resulting contraction in ≈18%) left the drill without any significant change in the holes geometry factors. As showed the EDAX analysis, the thermal treatment in air resulted that all the metallic nickel deposited on the drill wall was oxidized to NiO. Still, the obtained layer showed considerable difference to the rest of microstructure. The reduction step (Fig. 7c) left all the nickel in the material in metallic state including that in the drill walls. The microstructural observation of the drill wall (Fig. 7c) revealed that the sealing Ni layer generated in the green state presented elevated porosity similar to the whole microstructure of Ni–YSZ cermet.

4. Summary

Green ceramic machining showed superior performance if compared to the results observed with Ni–YSZ cermets and with the same NiO–YSZ ceramic in sintered state. High material removal performance can be attributed to the fact that at least

two processes are simultaneously present: thermal and mechanical ablation. The optimum ablation capacity pulse irradiance value was determined to be 6.9 GW/cm^2. Nevertheless, even the lowest pulse irradiance values of 0.56 GW/cm^2 resulted in very fast ablation rates and were selected for further works due to the smallest drill diameter generated.

Using the determined laser ablation parameters the NiO–YSZ ceramic pieces were machined to desired structures without observable changes within the microstructure of the final Ni–YSZ cermet.

Acknowledgements

The results were obtained under project financed by the Spanish Government: MAT2006-13005-C03-01. Jonas Gurauskis acknowledges the financial support provided by CSIC through I3P contract. Daniel Sola thanks to the University of Zaragoza and to BSH the financial support of his contract.

References

1. Imen, K. and Allen, S. D., Pulse CO_2 laser drilling of green alumina ceramic. *IEEE Trans. Adv. Pack.*, 1999, **22**(4), 620–623.
2. Dambra, D. M., Needes, M. C. A., Needes, C. R. S. and Wang, C. B., Via formation in green ceramic dielectrics using a YAG laser. In *Proceedings of the 42nd Electronic Components & Technology Conference*, 1992, pp. 1072–1081.
3. Knowles, M. R. H., Rutterford, G., Karnakis, D. and Ferguson, A., Micromachining of metals, ceramics and polymers using nanosecond lasers. *Int. J. Adv. Manuf. Technol.*, 2007, **33**(1–2), 95–102.
4. Otani, T., Herbst, L., Heglin, M., Govorkov, S. V. and Wiessner, A. O., Microdrilling and micromachining with diode-pumped solid-state lasers. *Appl. Phys. A: Mater.*, 2004, **79**(4–6), 1335–1339.
5. Guo, D., Cai, K., Yang, J. L. and Huang, Y., Spatter-free laser drilling of alumina ceramics based on gel casting technology. *J. Eur. Ceram. Soc.*, 2003, **23**(8), 1263–1267.
6. Nowak, K. M., Baker, H. J. and Hall, D. R., Cold processing of green state LTCC with a CO_2 laser. *Appl. Phys. A: Mater.*, 2006, **84**(3), 267–270.
7. Slocombe, A., Clarke, J. and Li, L., The effect of pigment addition in diode laser ablation machining of ceramic/polymer composite material. *Appl. Surf. Sci.*, 2000, **168**(1–4), 21–24.
8. Merino, R. I., Peña, J. I., Laguna-Bercero, M. A., Larrea, A. and Orera, V. M., Directionally solidified calcia stabilised zirconia–nickel oxide plates in anode supported solid oxide fuel cells. *J. Eur. Ceram. Soc.*, 2004, **24**(6), 1349–1353.
9. Orera, V. M., Peña, J. I., Laguna-Bercero, M. A., Merino, R. I. and Larrea, A., Ni and Co–ZrO_2 composites produced by laser zone melting. In *Ceramic Engineering and Science Proceedings of the 27th International Cocoa Beach Conference on Advanced Ceramics and Composites: B*, 2003, pp. 181–186.
10. Bäuerle, D., *Laser Processing and Chemistry*. Springer–Verlag, Berlin, 2000, p. 693.
11. Barin, I. and Platzki, G., *Thermochemical Data of Pure Substances*. VCH, Weinheim, Germany, 1995.
12. Leitner, J., Sedmidubsky, D. and Chuchvalec, P., Prediction of heat capacities of solid binary oxides from group contribution method. *Ceram.-Silikaty*, 2002, **46**(1), 29–32.
13. Watanabe, H., Thermal constants for Ni, NiO, MgO, MnO and CoO at low-temperatures. *Thermochim. Acta*, 1993, **218**, 365–372.